Pressure-induced superconducting state and effective mass enhancement near the antiferromagnetic quantum critical point of $CePt_2In_7$

E. D. Bauer, H. O. Lee, V. A. Sidorov,[*] N. Kurita, K. Gofryk, J.-X. Zhu, F. Ronning, R. Movshovich, and J. D. Thompson

Los Alamos National Laboratory, Los Alamos, New Mexico 87545, USA

Tuson Park[†]

Department of Physics, Sungkyunkwan University, Suwon 440-746, Korea

The heavy-fermion antiferromagnet $CePt_2In_7$ is a new, structurally more two-dimensional member of the $Ce_mM_nIn_{3m+2n}$ family. Applying pressure to $CePt_2In_7$ induces a broad dome of superconductivity that coexists with magnetic order for $1 \leq P \leq 3$ GPa. The maximum $T_c = 2.1$ K appears near the critical pressure $P_c = 3.5$ GPa where the Néel temperature extrapolates to zero temperature. An analysis of the initial slope of the upper critical field, the T^2 coefficient of the electrical resistivity, and specific heat indicates an enhancement of the effective mass m^* as P_c is approached, suggesting that critical fluctuations may mediate superconductivity. Electronic-structure calculations reveal a delicate balance between structural anisotropy and f-d hybridization, which may account for comparable T_c's in $CePt_2In_7$ and more three-dimensional $CeRhIn_5$.

Unconventional superconductivity in complex electronic d- and f-electron materials continues to be a subject of intense focus within the condensed-matter community. In the absence of a microscopic model for nonphononic mechanism(s) of unconventional superconductivity in which the pairing of electrons is mediated by magnetic, density, or valence fluctuations,[1] attention has been devoted to identify and investigate structural and other trends that generate (or enhance) superconductivity. It is well known that unconventional superconductivity is most often found in particular structural families; the highest T_c's occur in materials with two-dimensional (2D) structural units (e.g., CuO_2 planes in the cuprates or FeAs planes in the oxy-pnictide superconductors), indicating that reduced dimensionality is beneficial for unconventional superconductivity. Indeed, increasing the number of CuO_2 layers (up to 3) in the $HgSr_2Ca_{n-1}Cu_nO_{2n+2+\delta}$ systematically increases T_c from 97 to 135 K (e.g., Ref. [2]) and provides an effective means for enhancing superconductivity.

Several heavy-fermion compounds, such as $CeIn_3$ and $CePd_2Si_2$,[3] exhibit superconductivity as their Néel temperature is tuned by pressure toward a zero-temperature antiferromagnetic/paramagnetic boundary.[4] These observations have suggested that fluctuations associated with the magnetic quantum critical point (QCP) may provide the glue that binds Cooper pairs. In these materials, a dome of superconductivity emerges that is centered around P_c where $T_N \rightarrow 0$ and that evolves from an unusual normal state characterized by a non-Fermi-liquid-like temperature exponent of the electrical resistivity (i.e., $\rho \propto T^n$ with $n < 2$, instead of a Fermi-liquid $n=2$ exponent). Theoretical models suggest that antiferromagnetic fluctuations are most effective for generating d-wave superconductivity in a tetragonal crystal structure, which favors the attractive parts of the potential while minimizing the repulsive parts.[1] In these models, T_c depends on two factors:[1,5] a characteristic energy scale of the fluctuations, which depends sensitively on the hybridization between the f electrons and the conduction electrons in the

heavy-fermion materials, and the dimensionality of the system. With all other factors equal, the T_c of a 2D material will be higher than a three-dimensional one. To test these ideas in a controlled manner, it is desirable to have a family of structurally tunable heavy-fermion superconductors. In this Rapid Communication, we present the discovery of pressure-induced superconductivity in the heavy-fermion antiferromagnet $CePt_2In_7$, a new member of the $Ce_mM_nIn_{3m+2n}$ family whose crystal structure is more two dimensional than its $CeMIn_5$ cousins.[6] This new system is a model for testing relations among anisotropy, hybridization, and unconventional superconductivity.

Studies of the family of heavy-fermion $Ce_mM_nIn_{3m+2n}$ and $PuMGa_5$ ($M = Co, Rh, Ir$) superconductors already have found trends that support basic ideas of the theoretical model.[1] $CeMIn_5$, ($PuMGa_5$), and Ce_2MIn_8 materials crystallize in a tetragonal structure consisting of $CeIn_3$ ($PuGa_3$) planes (either $m=1$ or 2, respectively) separated by a single ($n=1$) MIn_2 layer stacked along the c axis. In the Ce members, structural tuning increases T_c from 0.2 K in cubic $CeIn_3$ to above 0.4 K in 218's (Refs. [7] and [8]) and to over 2 K in the quasi-2D 115's.[9–13] The characteristic energy scale T_0, a measure of the f-electron/conduction-electron hybridization, also appears to play an important role in setting the scale for T_c. This is most obvious in a comparison of the Pu- and Ce-based 115's where the greater radial extent of $5f$ wave function of Pu produces stronger hybridization and T_c's about an order of magnitude higher than in the Ce counterparts.[14] Within the Ce115 series, there also is the progression from antiferromagnetic ($M = Rh$) to superconducting with $T_c = 2.3$ K ($M = Co$) and 0.4 K ($M = Ir$). dynamical mean field theory calculations[15] show that chemistry drives this sequence from weak (Rh) to near optimal (Co) to "over" hybridization (Ir). Herein, we present an investigation of $CePt_2In_7$, the first $n=2$ member of the family, to explore the effects of reduced dimensionality, hybridization, and quantum critical fluctuations.

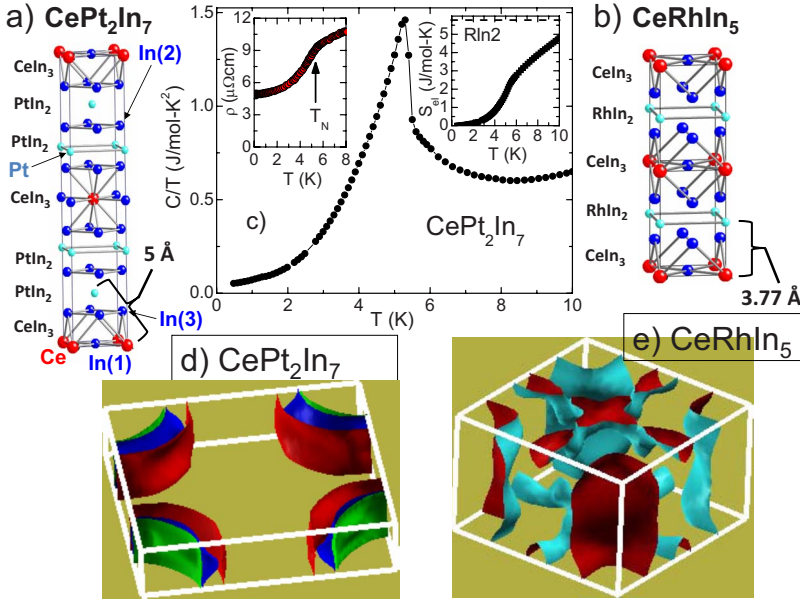Polycrystalline samples of $CePt_2In_7$ were prepared by arc-

FIG. 1. (Color online) Crystal structure of (a) $CePt_2In_7$ and (b) $CeRhIn_5$. (c) Specific heat C/T vs T of $CePt_2In_7$ of sample B. Right inset: entropy $S_{el}(T)$ below 10 K. Left inset: $\rho(T)$ below 8 K at 0.1 T. Band structure of (d) $CePt_2In_7$ and (e) $CeRhIn_5$. See text for details.

melting and the buttons were wrapped in Ta foil and annealed under vacuum at 500 °C for 2 weeks. X-ray diffraction measurements reveal the main phase is $CePt_2In_7$, which crystallizes in the body-centered $I4/mmm$ space group with lattice parameters $a=4.611(1)$ Å and $c=21.647(3)$ Å, consistent with a previous report.[16] Two samples were measured: sample A, in which extensive measurements of ac calorimetry were performed contained <2 vol % of $Ce_3Pt_4In_{13}$ impurities and sample B contained negligible amounts of $Ce_3Pt_4In_{13}$ and an unknown impurity phase. Specific heat, measured in a Quantum Design physical properties measurement system (PPMS) from 0.4 to 300 K, and electrical resistivity, performed via a standard four-wire measurement with Pt contacts, gave consistent results on both samples. ac-calorimetry measurements on sample A as a function of pressure were carried out as described in Ref. 12. The electronic structure was calculated using the WIEN2K package[17] and with the experimental lattice parameters as input. This package is a full-potential linearized augmented plane-wave method based on density-functional theory and uses the generalized gradient approximation for the exchange and correlation corrections. Nonoverlapping atomic-sphere radii of 2.5 (Ce), 2.5 (Rh), and 2.43 (In) atomic units were used for $CeRhIn_5$ while 2.5 (Ce), 2.5 (Co, Rh, Pd, Pt), and 2.39 (In) atomic units were used for CeM_2In_7. The Ce $4f$ states were treated as core states using criterion for the number of plane waves $R_{MT}K_{Max}=8$ and the number of k points of 1152 for $CeRhIn_5$ and 1600 for CeM_2In_7.

Figure 1(a) shows that the structure of $CePt_2In_7$ is comprised of a single $CeIn_3$ plane and two $PtIn_2$ layers stacked along the c axis of the tetragonal unit cell; this is a more two-dimensional variant of a new structure type in the $Ce_mM_nIn_{3m+2n}$ family. While the $CeIn_3$ block is similar to $CeMIn_5$, the Ce-Pt bond distance is much longer ($R_{Ce-Pt}=4.98$ Å) in this body-centered $CePt_2In_7$ structure than the Ce-M bond distance in the $CeMIn_5$ compounds ($R_{Ce-M}=3.77$ Å) [Fig. 1(b)], which decreases the f-d hybridization that has consequences for superconductivity as discussed below. The specific heat of $CePt_2In_7$, plotted as C/T vs T, is

displayed in Fig. 1(c). The peak at $T_N=5.5$ K is indicative of a second-order transition to an antiferromagnetic (AFM) state. A fit of the data to $C/T=\gamma+\beta T^2$ between $12<T<19$ K, yields $\gamma=340$ mJ/mol K^2 and $\beta=2.88$ mJ/mol K^4 (corresponding to a Debye temperature $\theta_D=189$ K). This Sommerfeld coefficient is similar to that of $CeRhIn_5$ (Ref. 12) and implies a large effective mass enhancement in $CePt_2In_7$. After subtraction of the βT^3 phonon term, the entropy amounts to $S_{el}\sim1/3R \ln(2)$ at the Néel transition [Fig. 1(c) inset]. Further evidence for the antiferromagnetic transition is provided by susceptibility measurements (not shown) and a change in slope at 5.5 K of the electrical resistivity $\rho(T)$ displayed in the inset of Fig. 1(c). A fit to the data for $T\ll T_N$ of $\rho(T)=\rho_0+AT^2$ yields $A=0.10$ $\mu\Omega$ cm/K^2. Assuming the Kadowaki-Woods relation,[18] this value of A implies a Sommerfeld coefficient $\gamma=100$ mJ/mol K^2, which is comparable to the extrapolated zero-temperature value of 50 mJ/mol K^2 in Fig. 1. This value of γ in the ordered state is about seven times smaller than $\gamma(T>T_N)$, which is typical of Ce-based magnets.[19] No superconductivity is found above 50 mK in $CePt_2In_7$ in 0.1 T at ambient pressure.

Figure 2 provides evidence for pressure-induced bulk superconductivity in $CePt_2In_7$ from ac-calorimetry measurements, plotted as C/T vs T at various pressures up to $P=3.53$ GPa as shown in Fig. 2(a) on sample A. The anomaly at $T_N=5.5$ K increases with pressure up to ~1.8 GPa, then decreases rapidly above that pressure such that only a broad anomaly is observed at 3 K at 3.12 GPa. Below 3 K, a single peak is found below 1 GPa due to the AFM transition of a $Ce_3Pt_4In_{13}$ impurity phase [Fig. 2(b)], which follows the monotonic behavior found previously up to 1.26 GPa.[20] Above 1 GPa, another peak attributed to bulk superconductivity is observed, the temperature of which increases monotonically with pressure from $T_c=1.2$ K (1.4 GPa) to 1.75 K (2.85 GPa) and the peak height remains small where there is coexistence with AFM order. Above 2.85 GPa, the superconducting anomaly increases up to $T_c=2.1$ K and the specific-heat jump ΔC is largest at 3.53 GPa where the Néel transition extrapolates to zero temperature.
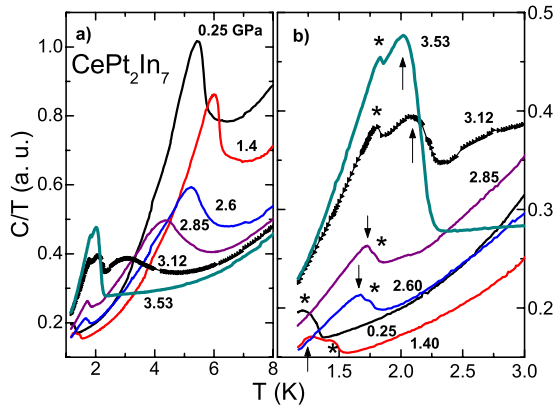
FIG. 2. (Color online) (a) ac calorimetry of $CePt_2In_7$ sample A, C/T vs T, up to 5 GPa and below 8 K and (b) below 3 K, showing the evolution of T_c in $CePt_2In_7$ (denoted by an arrow) and a $Ce_3Pt_4In_{13}$ impurity phase (*).

The temperature-pressure (T-P) phase diagram of $CePt_2In_7$ is shown in Fig. 3(a). The AFM transition first increases with pressure up to 1.5 GPa then decreases with increasing pressure and is absent once it intersects superconductivity. Superconductivity appears at ~1 K above 1 GPa and reaches a maximal value of T_c=2.1 K at P_c=3.5 GPa where $T_N(P)$ extrapolates to T=0 K. Electrical-resistivity measurements confirm a superconducting state and are generally consistent with the ac-calorimetry data. As with $CeRhIn_5$,[12] resistivity gives slightly higher T_c's when AFM order is present.

Several properties provide strong evidence for an enhancement of the effective mass near the antiferromagnetic
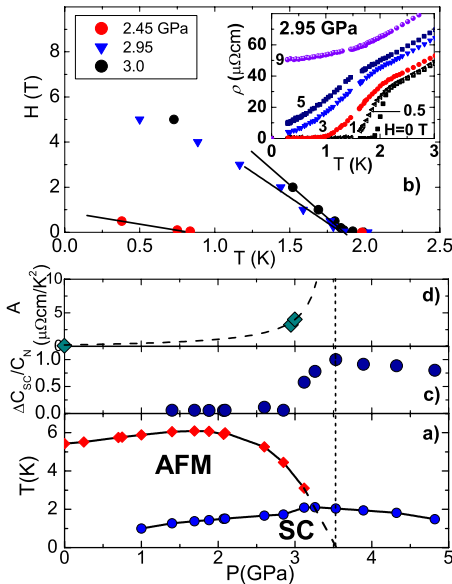

FIG. 3. (Color online) (a) P-T phase diagram of $CePt_2In_7$ constructed from calorimetry measurements. The dashed line is a guide to the eyes. (b) H-T phase diagram of $CePt_2In_7$ at various pressures. Inset: $\rho(H,T)$ curves used to determine T_c (midpoint of transition) and the H-T phase diagram. (c) Specific-heat jump ΔC_{SC} normalized to the value (C_N) just above T_c vs P. (d) T^2 coefficient, A, vs P at H=9 T.
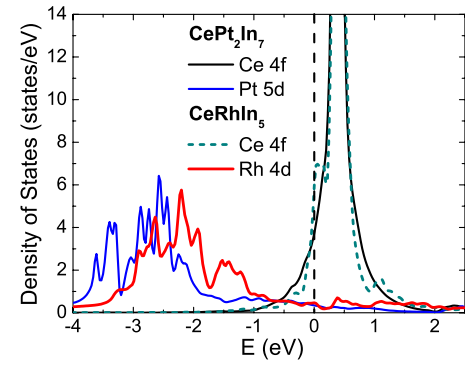

FIG. 4. (Color online) Ce $4f$, Rh $4d$, and Pt $5d$ DOS vs E for $CePt_2In_7$ and $CeRhIn_5$. See text for details.

quantum critical point in $CePt_2In_7$. Accompanying a large increase in the specific-heat jump at T_c, $\Delta C/C_N$, as $P \to P_c$ [Fig. 3(c)], the initial slope of the upper critical field $-dH_{c2}/dT_c$, from Fig. 3(b), is 1.08, 4.50, and 5.52 T/K at P=2.45 GPa, 2.95 GPa, and 3.0 GPa, respectively. With $-dH_{c2}/dT_c \propto m^{*2}T_c$, this implies that $m^* \sim 60m_e$, $80m_e$, and $90m_e$ in this pressure sequence.[21] In addition, as shown in Fig. 3(d) the normal-state T^2 coefficient of ρ increases rapidly upon approaching P_c, which is expected as a quantum critical point is approached.[4] At 3 GPa and 9 T [$>H_{c2}(0)$], A=4.03 $\mu\Omega$ cm/K^2, which is 40 times larger than the value at ambient pressure. From the Kadowaki-Woods ratio, this A implies γ=630 mJ/mol K^2, which is nearly twice the paramagnetic value at ambient pressure. We also note that this γ may be underestimated because A was determined in a high field.

The picture that emerges is that the effective mass of $CePt_2In_7$ is enhanced on approaching the antiferromagnetic quantum critical point at P_c=3.5 GPa. A broad dome of superconductivity with a maximum T_c of 2.1 K appears close to this critical pressure. The large initial slope of the upper critical field and specific-heat jump near P_c indicate intimate involvement of heavy quasiparticles in the superconductivity, and the remarkable similarity to $CeRhIn_5$ (Ref. 12) suggests that the superconductivity also is unconventional. As shown in Fig. 1(d), the calculated Fermi surface of $CePt_2In_7$ is comprised of three, nearly ideal cylindrical sheets, compared to corrugated cylindrical sheets in $CeRhIn_5$, one of which is shown in Fig. 1(e). Recent NMR measurements provide further evidence for the two-dimensional nature of $CePt_2In_7$ and the presence of 2D antiferromagnetic fluctuations above T_N.[22] Thus, it appears that 2D AFM critical fluctuations at the QCP dictate the behavior of $CePt_2In_7$.

Though the more two-dimensional crystal structure (and fluctuations) of $CePt_2In_7$ might be expected to lead to a higher T_c than in any $CeMIn_5$ material,[5] weaker f-d hybridization may limit the value of T_c in $CePt_2In_7$. Support for this possibility is provided by calculations comparing the density of states (DOS) of $CeRhIn_5$ and $CePt_2In_7$. The paramagnetic scalar-relativistic projected electron DOS vs E relative to the Fermi energy E_F for Ce $4f$, Rh $4d$, and Pt $5d$ is shown in Fig. 4. The Rh $4d$ and Pt $5d$ states are located about 2–3 eV below E_F, respectively, while the Ce $4f$ states are located 0.5 eV above E_F. The extra electron of Pt does not significantly

affect the band structure and only shifts E_F up by ~ 0.1 eV. There is some hybridization between Ce $4f$ and Rh $4d$, which produces a gap near E_F that is found as well in more sophisticated local-density approximation plus dynamical mean field theory calculations.[15] In contrast, hybridization between Ce $4f$ and Pt $5d$ is sufficiently weak to obscure a gap, if present at all. This difference is due in part to the larger nearest-neighbor Ce-M bond distance in CePt$_2$In$_7$ compared to that in CeRhIn$_5$, which may account in part for the higher pressure necessary to suppress magnetic order in CePt$_2$In$_7$.

An interesting question is whether higher T_c's might be found in other hypothetical CeM_2In$_7$ ($M=$Co,Rh,Pd,Pt) compounds. In the Ce115 family, the transition metal tunes hybridization between the $4f$ and out-of-plane In, which appears to be a dominating factor.[15] In the Ce127 structure, the In(3) site plays the equivalent role (Fig. 1), and we consider specifically the effect that the In(3) bandwidth might have on T_c. A Lorentzian fit to the In(3) DOS (not shown) yields a bandwidth $W^{In(3)}$ of 3.6 eV, 5.9 eV, 4.1 eV, and 5.0 eV for $M=$Co, Rh, Pd, and Pt, respectively. Hybridization of Ce f and In p electrons will broaden the f level to a width $\Gamma = \pi \langle V_{kf}^2 \rangle N_p^{eff}(E_F)$ in the Kondo limit, where V_{kf}^2 is the matrix element that mixes f-electron/conduction-electron states. As argued earlier,[14,23] Γ sets the energy scale for superconductivity in families of strongly correlated systems, i.e., $\Gamma \propto T_0 \propto T_c$. Assuming $\langle V_{kf}^2 \rangle$ is a constant in this structure and that

$N_p^{eff}(E_F) \sim 1/W^{In(3)}$, then from the relation $T_c \propto T_0$,[14] we expect a higher T_c for $M=$Co and Pd and a lower T_c for M $=$Rh (relative to 2.1 K in CePt$_2$In$_7$). These very qualitative estimates suggest that the hybridization and anisotropy may be further optimized in these two-dimensional CeM_2In$_7$. More realistic calculations and the search for additional CeM_2In$_7$ materials are worthwhile.

In summary, the heavy electron antiferromagnet CePt$_2$In$_7$ is a new, more two-dimensional member of the Ce$_m M_n$In$_{3m+2n}$ family. Bulk superconductivity with a maximum transition temperature $T_c=2.1$ K is induced as magnetic order is tuned toward an antiferromagnetic quantum critical point at a critical pressure $P_c=3.5$ GPa. An analysis of physical properties reveals an enhancement of the effective mass near the QCP, possibly associated with 2D AFM fluctuations. Electronic-structure calculations indicate relatively weaker f-d hybridization in CePt$_2$In$_7$ compared to CeRhIn$_5$ but greater anisotropy in the 127 structure compensates this effect to give a comparable T_c in both systems. Further enhancement of T_c may be found in other CeM_2In$_7$ materials.

*Also at Institute for High Pressure Physics, Russian Academy of Sciences, 142190 Troitsk, Russia.

†Also at Los Alamos National Laboratory, Los Alamos, New Mexico 87545, USA.

[1] P. Monthoux, D. Pines, and G. G. Lonzarich, Nature (London) **450**, 1177 (2007).

[2] See, for example, Ø. Fischer *et al.*, Rev. Mod. Phys. **79**, 353 (2007).

[3] N. D. Mathur *et al.*, Nature (London) **394**, 39 (1998).

[4] G. R. Stewart, Rev. Mod. Phys. **73**, 797 (2001).

[5] P. Monthoux and G. G. Lonzarich, Phys. Rev. B **59**, 14598 (1999).

[6] A preliminary report of this work was presented at the International Conference on Magnetism, 2009 [E. D. Bauer *et al.*, J. Phys.: Conf. Ser. (to be published)].

[7] D. Kaczorowski, A. P. Pikul, D. Gnida, and V. H. Tran, Phys. Rev. Lett. **103**, 027003 (2009).

[8] J. D. Thompson *et al.*, Physica B **329-333**, 446 (2003).

[9] C. Petrovic *et al.*, J. Phys.: Condens. Matter **13**, L337 (2001).

[10] J. L. Sarrao *et al.*, Nature (London) **420**, 297 (2002).

[11] H. Hegger, C. Petrovic, E. G. Moshopoulou, M. F. Hundley, J. L. Sarrao, Z. Fisk, and J. D. Thompson, Phys. Rev. Lett. **84**, 4986 (2000).

[12] T. Park *et al.*, Nature (London) **440**, 65 (2006).

[13] J. D. Thompson *et al.*, J. Alloys Compd. **408-412**, 16 (2006).

[14] N. J. Curro *et al.*, Nature (London) **434**, 622 (2005).

[15] K. Haule, C. Yee, and K. Kim, arXiv:0907.0195 (unpublished).

[16] Z. Kurenbaeva *et al.*, Intermetallics **16**, 979 (2008).

[17] P. Blaha, K. Schwarz, G. Madsen, D. Kvasnicka, and J. Luitz, in *WIEN2k, An Augmented Plane Wave Plus Local Orbitals Program for Calculating Crystal Properties*, edited by K. Schwarz (Technische Universität Wien, Austria, 2001).

[18] K. Kadowaki and S. B. Woods, Solid State Commun. **58**, 507 (1986).

[19] Z. Fisk *et al.*, Science **239**, 33 (1988).

[20] M. F. Hundley, J. L. Sarrao, J. D. Thompson, R. Movshovich, M. Jaime, C. Petrovic, and Z. Fisk, Phys. Rev. B **65**, 024401 (2001).

[21] T. P. Orlando, E. J. McNiff, S. Foner, and M. R. Beasley, Phys. Rev. B **19**, 4545 (1979).

[22] N. apRoberts-Warren, A. Dioguardi, A. Shockley, C. Lin, J. Crocker, P. Klavins, and N. Curro, arXiv:1002.3204 (unpublished).

[23] J. D. Thompson *et al.*, J. Alloys Compd. **444-445**, 19 (2007).